Dynamics of Nondilute Hairy-Rod Polymer Solutions in Simple Shear Flow

Loic Hilliou and Dimitris Vlassopoulos*

Foundation for Research and Technology−Hellas (FO.R.T.H.), Institute of Electronic Structure and Laser, P.O. Box 1527, 71110 Heraklion, Crete, Greece

Matthias Rehahn

Institut für Makromoleculare Chemie und Deutsches Kunststoff Institut, Technische Universität Darmstadt, D-64287 Darmstadt, Germany

Received November 8, 2000

ABSTRACT: We investigate the shear response of nondilute solutions of a hairy-rod polyester using in-situ optical rheometry. The transition to the concentrated regime, c^{**}, is characterized by a strong concentration dependence of the zero shear viscosity, a change in the sign of birefringence, and the emergence of linear conservative dichroism. These features indicate the presence of clusters which dominate the dynamics in this concentration regime, and as such they represent their identifying signature. The stress−optical rule is found to hold only in the concentration regime below c^{**}, yielding stress−optical coefficients closer to those of flexible chains rather than rods, consistent with the wormlike character of the polyesters. At the highest concentrations these solutions can be viewed as nondilute solutions of flexible ellipsoidal clusters. The dynamics as well as the anomalous birefringence (change of sign) can be rationalized using the theoretical analysis of Cates, who considered a presmectic local ordering resulting from the interplay of sterically interacting particles and the external field.

I. Introduction

Hairy-rod polymers (thereafter abbreviated as HRP's) are now established as a class of highly anisotropic synthetic wormlike polymers with relatively low persistence length (compared to conventional rodlike polymers such as PBLG or xanthan gum)[1,2] and a number of potential technologically viable applications, especially in devices for micromechanics, molecular electronics, and information storage.[3] Consequently, understanding the fundamentals of their processing behavior will advance both their applicability and the molecular design and tailoring of such materials through knowledge of their microstructure−macroscopic properties interplay.[4,5]

In recent years we focused on the elucidation of the equilibrium dynamics of HRP's in solution by considering all three concentration regimes, namely dilute, semidilute, and concentrated.[6−8] In particular, using model polyesters and poly(*p*-phenylenes) bearing aliphatic side chains,[3,9] we have explored their dynamics of association under equilibrium conditions using photon correlation spectroscopy.[6] These polymers constitute a special class of semiflexible macromolecules with a large inherent optical anisotropy due to the phenyl rings and a conformation described by the wormlike chain model, as demonstrated by depolarized Rayleigh scattering experiments;[8] they form aggregates in solution even at low concentrations due to side-chain crystallization,[6] and their dynamics at high concentrations is dominated by the cluster response, displaying signs of pretransitional local ordering, i.e., orientational correlations.[6,7]

Concerning the relation of the properties of these materials to their processing, which is important for various applications, understanding of the dynamics of sheared solutions, and in particular the flow-induced orientation or structure formation, is of prime importance. In this respect, the established efficiency of rheo-optical techniques[10] in probing the effects of shear (for example, in inducing anisotropy and orientation) in a variety of complex fluids, including rodlike polymers,[11] provides the appropriate experimental vehicle for carrying out these investigations with HRP's.

HPR's already investigated with rheo-optics include poly(*n*-hexyl isocyanate)[12] and poly(*p*-phenylenes).[5,13] All are quite polydisperse in size and exhibit a tendency to form aggregates in solution, which essentially coexist with wormlike chains.[6,12] The latter systems represent a continuation of our above-mentioned longstanding program on the dynamics of well-characterized HRP's. The main findings from these studies suggest the presence of a two-step decay characterizing the relaxation of birefringence relating to different cluster sizes; the orientation of the formed aggregates in a direction perpendicular to the flow field with their constituents oriented along the flow.[5,12,13] An explanation of this remarkable effect calls for a kind of pretransitional smecticlike ordering resulting from the coupling of the external field and the steric interactions of the polymers.[14]

In this paper we extend the above work by studying systematically the effects of concentration, which have not been addressed before, on the dynamic response of solutions of a model wormlike hairy-rod polyester subjected to a simple shear flow. We find that the transition to the concentrated regime is characterized by a strong concentration dependence of the zero-shear viscosity, a change in the sign of the birefringence, and the emergence of linear conservative dichroism. Using information in both the flow-velocity gradient and flow-vorticity planes, we propose a picture of the shear-induced dynamics of these solutions in different concentration regimes.

10.1021/ma001917l CCC: $20.00
Published on Web 02/16/2001

Scheme 1. Molecular Structure of the Poly(*p*-terphenylene terephthalate) Molecules with Hexyl Side Chains (Hairs), TPPE

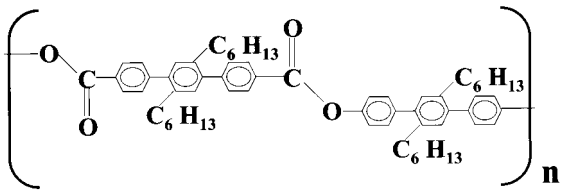

II. Experimental Section

Materials. The synthesis and characterization of a series of hairy-rod polyesters, namely poly(*p*-terphenylene terephthalates), abbreviated as TPPE, is described in detail elsewhere.[9] The molecular structure of the TPPE's bearing hexyl side chains, used in this work, is shown in Scheme 1, whereas its number-average molecular weight is $M_n = 18\,000$ g/mol and its polydispersity about 1.7. For this polymer, the number-average countour length is $L_n = 64.4$ nm, and its persistence length is typically $l = 20$ nm, typical of wormlike chain conformation.[8] The overlap concentration ($c^* = 0.09$ wt %) was determined from light scattering measurements at different concentrations.[13] The onset of the concentrated regime is marked by the concentration $c^{**} \sim b^{-1}L_e^{-2}$, with $b \approx 1.2$ nm the average diameter of the molecule and $L_e = 42$ nm the effective contour length defined as[1]

$$L_e = \left(2l^2\left[\frac{L_n}{l} - 1 + \exp\left(-\frac{L_n}{l}\right)\right]\right)^{1/2} \qquad (1)$$

c^{**} was estimated to be around 2.5 wt %. The various solutions were prepared in tetrachloroethane, a good solvent with relatively high boiling point (140 °C) to reduce evaporation problems, and density $\rho = 1.6$ g/mL, by adding the polymer to the solvent under strong stirring at 80 °C for 12 h. All solutions were used fresh; i.e., immediately after this treatment, they were cooled to 25 °C and loaded into the rheometer. In this way, the aging problem and its consequences were not a concern.[13] The concentrations examined covered the range 0.36−7.24 wt %. This range was the widest experimentally accessible as the solutions gelled at higher concentrations, whereas limitations in torque resolution of the rheometer prevented measurements at lower concentrations.

Methods: Mechanical and Optical Rheometry. Simultaneous measurements of viscoelastic and optical properties of the TPPE solutions were carried out by combining a Rheometric Scientific constant stress rheometer (DSR-200) with an optical train.[5] The latter includes a He−Ne laser generating a coherent polarized beam of power 5 mW at wavelength $\lambda = 632.8$ nm, which passes through the polarization state generator (PSG), the flow cell, and the polarization state analyzer (PSA). The PSG includes a polarizer, a photoelastic modulator (PEM) operating at a frequency of 50 kHz, and a quarter wave plate, with respective orientations 0°, 45°, and 0°, relative to the laboratory frame, and net result a linearly polarized light (with orientation oscillating at 50 kHz and amplitude prescribed by the PEM) exiting the PSG.

Two flow cells were employed (see Scheme 2). The first consisted of two parallel quartz plates (measuring optical anisotropy in the flow-vorticity plane) of diameter 38.1 mm, with the sample loaded between them (the sample thickness was 1 mm); the second was a Couette cell (measuring optical anisotropy in the flow-velocity gradient plane) consisting of two coaxial cylinders with height of 44 mm and gap of 2.6 mm and with the bottom of the outer cylinder (with inner diameter 32 mm) made of quartz glass to allow light passing through.

The PSA consists of a circular polarizer (CP) and a photodiode. When the CP is in the optical path, this configuration measures the birefringence ($\Delta n'$); actually, it measures the difference of $\Delta n'$ from dichroism, but the contribution of the latter is considered insignificant in the present discussion. On the other hand, when the CP is removed, the measurement

Scheme 2. Representation of the Flow Geometry Used along with the Principal Axes of the Refractive Index Ellipsoid: (a) Parallel Plates; (b) Couette

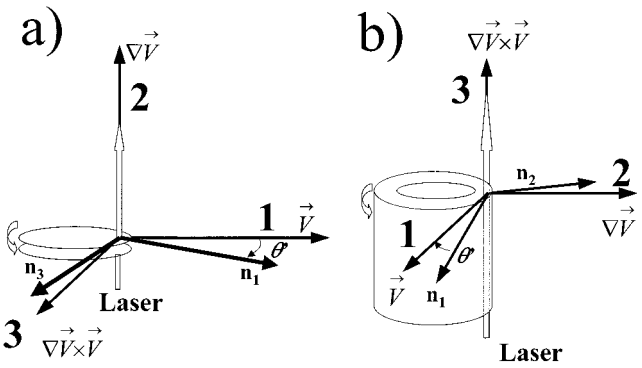

provides directly the dichroism ($\Delta n''$). In this work, the dichroism signal could only be detected when the Couette cell was utilized; its origin was the enhanced scattering as the polymers did not absorb at the wavelength utilized and thus related to the presence of aggregates.

The Fourier expansion of the transmitted intensity in the photodiode is $I = I_{DC} + I_\omega \sin(\omega t) + I_{2\omega} \cos(2\omega t) + ...$, where I_{DC} is the DC component, ω is the frequency of the PEM, and the amplitudes of the first and second harmonics, I_ω and $I_{2\omega}$, respectively, are given by (when the circular polarizer is in the optical train)

$$I_\omega = I_\omega^B = I_{DC}\, R_\omega^B = -2I_{DC}\, J_1 \cos 2\chi' \sin \delta' \qquad (2)$$

$$I_{2\omega} = I_{2\omega}^B = I_{DC} R_{2\omega}^B = I_{DC}\, J_2 \sin 2\chi' \sin \delta' \qquad (3)$$

with the parameters J_1 and J_2 being the calibration constants of the Fourier decomposition (Bessel function coefficients), determined experimentally, and the angle χ' defining the orientation of the principal direction of the refractive index tensor in the plane orthogonal to the axis of light propagation, relative to the polarizer direction. In such a case, the orientation angle relative to the flow direction is $\theta' = \chi' - 45°$. In eqs 2 and 3, contributions arising from the dichroism are considered to be small and are neglected (see also the discussion section below).

For the parallel plates flow geometry, the angle θ' is 0° or 90° due to symmetry considerations.[10] The retardation δ' relates to the birefringence $\Delta n'$ in the same plane (defined by the vorticity and flow directions) through $\delta' = 2\pi\Delta n' d/\lambda$, with d being the optical path length. Using the normalized intensities R_ω^B and $R_{2\omega}^B$, measured in two lock-in amplifiers ("locked" at ω and 2ω, respectively), and with sampling times varying between 50 and 500 ms, we can calculate directly δ' and χ' from eqs 2 and 3. When the Couette geometry is used, the birefringence $\Delta n'$ is measured in the plane of the flow and velocity gradient directions. In that plane, the birefringence orientation angle θ' can take any value between 0° (alignment with the flow) and 90° (alignment with the velocity gradient). Most of the optical measurements were performed in the parallel plate geometry (largely due to limitations in the sample availability), and only a limited number was performed in the Couette geometry to detect θ' as well as the dichroism, as will be explained below.

When the circular polarizer is removed from the optical train, the dichroism is measured, and the amplitudes of the first and second harmonics of the Fourier expansion of the intensity read

$$I_\omega = I_\omega^D = I_{DC} R_\omega^D = -2I_{DC} J_1 \sin 2\chi'' \tanh \delta'' \qquad (4)$$

$$I_\omega = I_{2\omega}^D = I_{DC} R_{2\omega}^D = -2I_{DC} J_1 \cos 2\chi'' \tanh \delta'' \qquad (5)$$

with χ'' being the orientation angle of the dichroism, relative to the polarizer, and δ'' the extinction of the light, related to

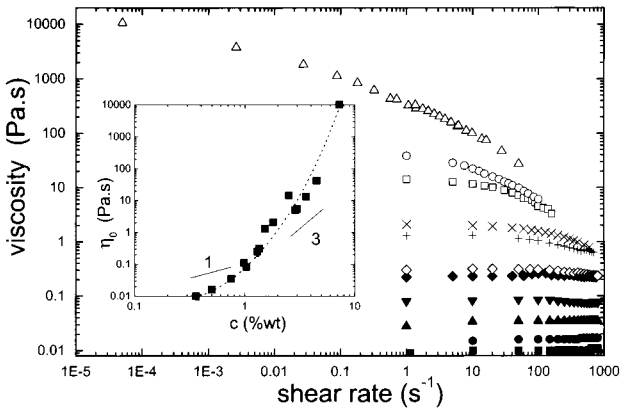

Figure 1. Steady shear viscosities of TPPE solutions at different concentrations (0.35 wt %, ■; 0.5 wt %, ●; 0.75 wt %, ▲; 1 wt %, ▼; 1.3 wt %, ◆; 1.4 wt %, ◇; 1.5 wt %, +; 1.8 wt %, ×; 2.5 wt %, □; 4.5 wt %, ○; 7.2 wt %, △). Inset: concentration dependence of the zero-shear viscosity. Slopes 1 and 3 indicate the dilute and semidilute scalings for semiflexible polymers, respectively (see text). The dotted line is drawn to guide the eye.

the dichroism through $\delta'' = 2\pi\Delta n'' d/\lambda$. The dichroism orientation angle relative to the flow direction is given by $\theta'' = \chi'' - 45°$.

Rheological measurements included step and steady rate sweep tests, which were carried out with the controlled strain option, in the shear rate range $1-1000\ s^{-1}$. The temperature was maintained at 25 °C using the original DSR recirculating fluids bath, appropriately modified in order to fit in the optical train.[5]

III. Results and Discussion

III.1. Rheology. Figure 1 represents the rheograms of TPPE, depicting the shear rate dependent viscosity at various concentrations. For $c > c^{**}$ a weak shear thinning is observed at high shear rates; this suggests rather fast relaxation times, which increase with increasing concentration, as expected. Note that these times compare well with the birefringence relaxation times discussed later on (in conjunction with Figure 6). At the highest concentration (7.2 wt %), the Newtonian plateau is barely reached. The extracted zero-shear viscosity η_0 is plotted against concentration in the inset of Figure 1. It is evident that the data points follow a curve that is concave upward, suggesting that no simple power laws can describe them; this type of behavior is typical for semiflexible polymer solutions.[2] The solid lines with slopes 1 and 3 represent the expected scaling laws for dilute and semidilute solutions of rods, respectively.[3,15] The strong concentration dependence suggests intermolecular interactions, in addition to the contributions of clusters which are present in this case.[13] An attempt to fit such a type of viscosity−concentration curve by accounting explicitly for the different contributions to the viscosity in the framework of the fuzzy cylinder model was presented recently for a series of substituted poly(*p*-phenylenes).[16] At the highest concentration in the present polyesters the gelation threshold is reached; note that a lyotropic mesophase was never observed. Note also that at concentrations above 1 wt % a tendency for crossing of the shear viscosity curves is observed, which might be indicative of the nonlinear coupling between the shear field and the strong excluded volume interactions in this regime.[15] Such a behavior was observed in concentrated isotropic solutions of rodlike poly(benzyl L-glutamate);[17] on the other hand, in the present systems as clusters apparently suppress the tendency for mesophase formation, no critical slowing down and jamming of the hairy rods are seen.

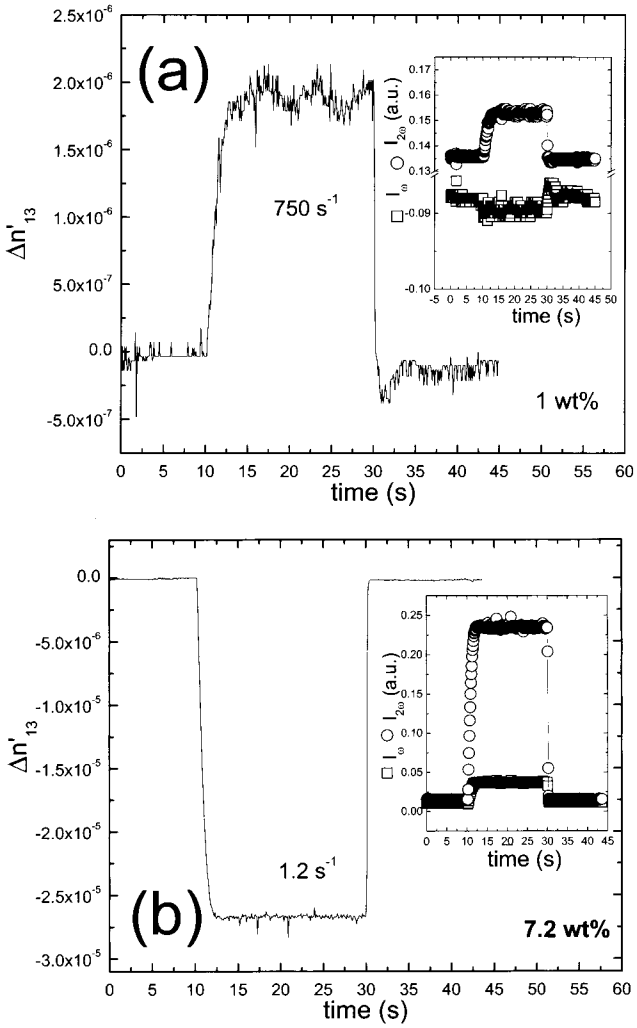

Figure 2. Transient birefringence $\Delta n_{13}'$ of two TPPE solutions in tetrachloroethane, along with the respective I_ω (□) and $I_{2\omega}$ (○) signals, shown in insets: (a) 1 wt %, at $\dot\gamma = 750\ s^{-1}$; (b) 7.2 wt %, at $\dot\gamma = 1.2\ s^{-1}$.

III.2. Shear-Induced Birefringence in the Flow-Vorticity Plane: Parallel Plate Experiments. a. Transients. A typical transient behavior of the induced birefringence during the application of a step rate for a duration of 20 s in 1 wt % ($\dot\gamma = 750\ s^{-1}$) and 7.2 wt % ($\dot\gamma = 1.2\ s^{-1}$) TPPE solutions is shown in Figure 2. It is evident that whereas for the lower concentration $\Delta n' > 0$, for the higher concentration the sign is reversed. This can be unambiguously deduced from the I_ω and $I_{2\omega}$ signals shown in the insets of Figure 2. In the former case, the birefringence orientation angle of the trimers or small anisotropic clusters is 0°, i.e., along the flow direction; on the other hand, in the latter case, the orientation angle of the clusters is perpendicular to the flow (−90°). This situation has been analyzed in refs 5 and 13, which by invoking the theory of Cates[14] attributed this "anomalous birefringence" behavior to a kind of pretransitional local ordering resulting from the interplay of the steric forces and the flow field. It is interesting to note that, based on the characterization discussed above, the 1 wt % solution (Figure 2a) is around c^{**} whereas the 7.2 wt % solution (Figure 2b)

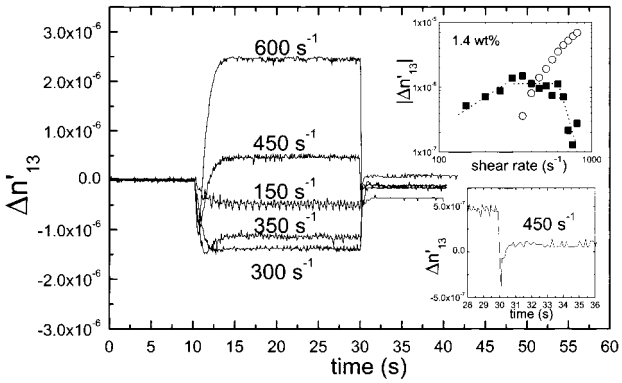

Figure 3. Transient flow-induced birefringence $\Delta n_{13}'$ for a 1.4 wt % TPPE solution at different shear rates ranging from 150 to 600 s^{-1}. Upper inset: absolute values of the extracted processes (negative birefringence, ■; positive birefringence, ○). The dotted lines are drawn to guide the eye (see text). Lower inset: magnification of the birefringence relaxation at 450 s^{-1}, indicating the negative values at short times.

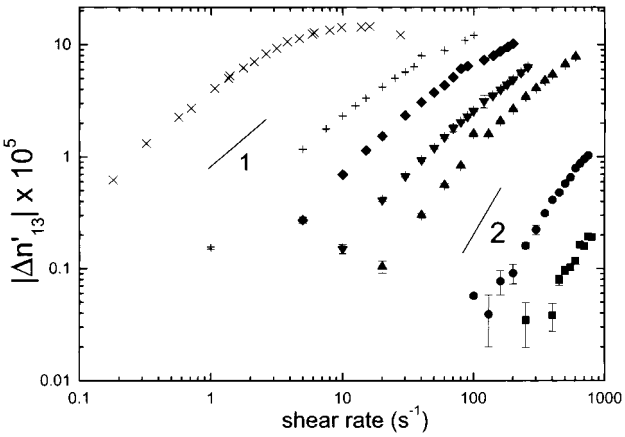

Figure 4. Shear rate dependence of the absolute value of the steady-state flow birefringence at different concentrations: 1 wt %, ■; 1.3 wt %, ●; 1.8 wt %, ▲; 2.9 wt %, ▼; 3.6 wt %, ◆; 4.5 wt %, +; 7.2 wt %, ×.

is clearly above c^{**}. The estimated transition from positive to negative birefrigence is 1.4 wt %, which is not so far below the c^{**} (given also the error involved in the c^{**} estimation); it can be concluded, therefore, that the concentrated regime is characterized by the change of sign of birefringence. Based on Cates' theory,[14] the birefringence anomaly is predicted to occur at concentrations where the sterically interacting ellipsoids start to overlap; with the onset of overlap of small clusters (or trimers) being characterized by c^{**}, then the occurrence of the transition in sign of birefringence for TPPE can be explained by this theory.

As the transition from positive to negative birefringence apparently relates to the formation of aggregates, on the basis of the above discussion, the inverse transition should represent a signature of cluster breakup. Indeed, this is demonstrated in Figure 3, which depicts the transient flow-induced birefringence at various shear rates for a 1.4 wt % solution. At low shear rates the negative birefringence probes the presence of clusters; its magnitude increases with shear rate. The extracted contributions to the overall birefringence are shown in the upper inset of Figure 3. At intermediate shear rates a negative birefringence first develops upon inception of the shear flow, followed by a positive birefringence. At higher shear rates, the overall birefringence is positive, but its relaxation upon cessation of shear is complex, exhibiting both positive (fast) and negative (slow) components (see also lower inset of Figure 3). A similar behavior is also discussed in conjunction with the Couette flow experiments and Figures 7 and 8.

A tentative explanation for the observed transition is presented here: For the present 1.4 wt % solution, dynamic light scattering[6,7,18] data suggest that trimers (or small anisotropic clusters) are in equilibrium with large clusters. As already discussed elsewhere,[12] upon inception of shear the larger anisotropic species will orient first and contribute to a negative birefringence associated with a cluster orientation angle along the vorticity direction. This is easily explained in the simple case of rods; the larger the rod, the less shear is needed to orient it.[11a] In the present case we are dealing with species having different aspect ratios (trimers vs larger clusters), and therefore we suggest that the clusters (with less overall optical anisotropy and thus birefringence) will orient first under shear.

The negative birefringence contribution saturates at not so high shear rates, as expected from theoretical arguments;[14] for the specific example of the 1.4 wt % solution, this occurs at $\dot{\gamma} \approx 350$ s^{-1} (see the upper inset of Figure 3). Since this birefringence anomaly depends on the orientation of (few) clusters made of many polymers (see below), one expects the corresponding birefringence to saturate easily.[14] At high shear rates small clusters or trimers orient in the velocity direction giving rise to positive birefringence. It is also quite likely that at high shear rates the mechanical energy induced to the sample may break up or significantly deform the aggregates, giving rise to positive overall birefringence because of the sharp drop of the negative birefringence contribution (upper inset of Figure 3). Such a situation normally corresponds to a macroscopic shear thinning behavior; actually, the weak but unambiguous drop of shear viscosity for the 1.4 wt % solution at $\dot{\gamma} > 200$ s^{-1}, observed in Figure 1, conforms to this picture. It is interesting, however, that the shear-induced breakup and reorganization of the cluster suspension has a much more pronounced optical effect, as seen in the birefringence measured at the velocity−vorticity plane (upper inset of Figure 3) compared to its influence on the macroscopic properties (Figure 1).

Further support for the cluster breakup senario comes from theoretical predictions,[14] which were confirmed by experimental observations in polyelectrolyte and surfactant solutions,[19] on the anomalous electric birefringence behavior of presmectic clusters. According to the theory, the birefringence relaxation is a two-step decay, with a fast positive and a slow negative processes. The negative birefringence, which appears at $c \gg c^*$, is associated with long relaxation times and resolved at small enough external field, where clusters are not destroyed. Its saturation is reached easily and reflects the orientation of the clusters.

b. Steady-State Behavior. The shear rate dependence of the steady-state birefringence is depicted for various concentrations in Figure 4. Whereas the lower concentrations regime is characterized by a positive shear-induced birefringence with scaling $\Delta n' \sim \dot{\gamma}^2$, above a critical concentration of 1.3 wt %, a negative birefringence emerges; the scaling of the positive $\Delta n'$ suggests the validity of the stress−optical rule as discussed below. Note that, as already mentioned, the overall birefringence measured during the application of steady

shear flow results from two different contributions: that arising from the trimers or small clusters (positive birefringence) and that relating to the presmectic aggregates (negative birefringence). The magnitude of the negative birefringence follows the scaling $\Delta n'_{13} \sim \dot{\gamma}$ at lower shear rates, whereas at the higher shear rates the scaling exponents are clearly recuded for all concentrations $c \geq 1.8$ wt %, suggesting the possible breakup of clusters,[5] also conforming to the observed shear thinning behavior of Figure 1.

c. Stress−Optical Rule Considerations. Under certain conditions, the stress−optical rule (SOR) can be considered for the parallel plate geometry employed.[20] It is well-known that the stress−optical rule assumes the coincidence of the principal directions of the stress and the refractive index ellipsoids, implying that the measurements are taken in the linear regime. In such a case the following equations hold:[10]

$$n_{ij} = C\sigma_{ij} \quad \text{and} \quad \theta = \theta' \tag{6}$$

where θ is the angle between the flow direction and the principal stress axis in the flow plane, θ' is the extinction angle resolved in the flow plane, i.e., the angle between the flow direction and the principal axis of the refractive index ellipsoid, and C is the stress−optical coefficient. For the simple shear flow of Scheme 2a, this can be written as

$$\sigma_{12} = \Delta n'_{12} \sin 2\theta / 2C \tag{7}$$

$$N_1 = \Delta n'_{12} \cos 2\theta / C \tag{8}$$

$$N_1 = \Delta n'_{23}/C = (\Delta n'_{13} - \Delta n'_{12} \cos 2\theta)/C \tag{9}$$

where N_1 and N_2 are the first and second normal stress differences, respectively. Under the assumption that $\Delta n'_{23}$ is vanishingly small, we end up with[20]

$$\Delta n'_{13} - \Delta n'_{12} \cos 2\theta \tag{10}$$

In fact, $\Delta n'_{13}$ is the measured quantity during an experiment with the parallel plate geometry. On the other hand, the same experiment probes the "12" component of the stress tensor (Scheme 2a), $\sigma_{12} = \eta\dot{\gamma}$. A combination of eqs 7 and 10 yields

$$\Delta n'_{13} = 2C\sigma_{12} \operatorname{cotan} 2\theta \tag{11}$$

The trigonometric term in the above equation can be expressed in terms of the shear rate. On the basis of the expected scaling $N_1 \sim \dot{\gamma}^2$ for concentrated solutions,[21] from eqs 7 and 8 we get cotan $2\theta \sim \dot{\gamma}^2$. Therefore, the measured flow birefringence scales with shear rate according to the following equation:

$$\Delta n'_{13} = 2C\eta_0\tau_c\dot{\gamma}^2 \tag{12}$$

where τ_c is the characteristic longest relaxation time, typically associated with the onset of shear thinning (if one can measure it in the appropriate shear rate range). A test of the validity of eq 12 is presented in Figure 5, which depicts the steady-state birefringence as a function of the square of the shear rate for different TPPE concentrations. It is evident that eq 12 is satisfied for the 1 and 1.3 wt % solutions (below c^{**}), exhibiting a positive value of the detected birefringence and a Newtonian viscosity. Therefore, for these two solutions

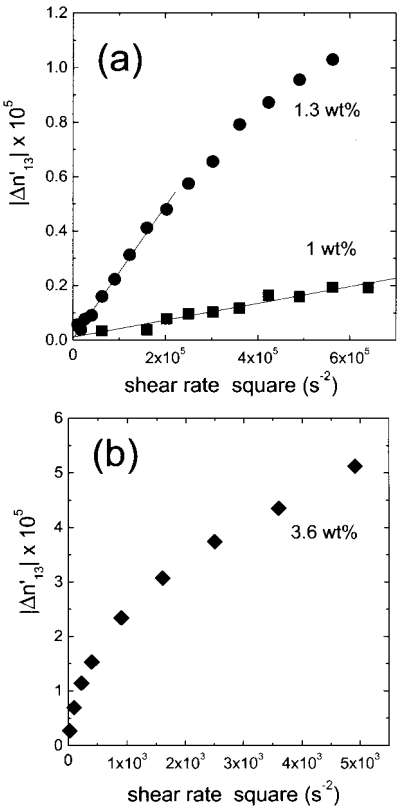

Figure 5. Steady-state birefringence $\Delta n_{13}'$ (absolute values) as a function of $\dot{\gamma}^2$ at different concentrations: (a) 1 wt %, ■; 1.3 wt %, ●; (b) 3.6 wt %, ◆.

the SOR seems to be valid. A rough estimation of the stress−optical coefficient (because it is not possible to determine precisely $\tau_c = \dot{\gamma}_c^{-1}$, based on Figure 1, where $\dot{\gamma}_c^{-1}$ corresponds to the onset of shear thinning) yields respective values of $C > 2 \times 10^{-8}$ Pa^{-1} (obtained with $\tau_c < 10^{-3}$ and zero-shear viscosity $\eta_0 = 0.085$ Pa·s) and $C > 5 \times 10^{-8}$ Pa^{-1} (obtained with $\tau_c < 10^{-3}$ s and $\eta_0 = 0.23$ Pa·s). For lower concentrations the birefringence could not be accurately resolved, whereas for higher concentrations its sign was negative, apparently due to the dominance of clusters.[5]

It should be noted that for rigid-rod polymers C is reported to be an increasing function of the molecular weight, and it is expected to increase with concentration as the isotropic-to-nematic transition is approached.[17] On the other hand, for flexible polymers C is virtually independent of both molecular weight and concentration.[15] Further, the value of C is about 3 orders of magnitude higher for rods compared to flexible coils; typically, Mead and Larson[17] have reported C values for PBLG ($M_w = 230\,000$ g/mol) and polystyrene ($M_w = 8 \times 10^6$ g/mol) of 10^{-6} and 10^{-9} Pa^{-1}, respectively. In this respect, our estimated values suggest that the polyesters investigated exhibit behavior resembling flexible rather that rigid-rod polymeric character. This is not surprising, considering the rather low persistence length of these semiflexible polymers, which are described by the wormlike chain model.[8] It is further noted that we cannot exclude the possibility of probing trimers or small clusters which are flexible, and in this respect the present results are in qualitative agreement with earlier investigations of Gatzonis et al.[12] on wormlike chains.

d. Birefringence Relaxation. The birefringence relaxation times upon flow cessation were analyzed with

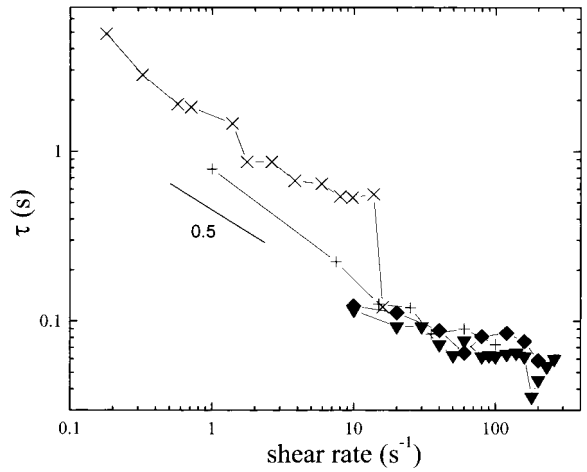

Figure 6. Birefringence relaxation times (τ) upon flow cessation: 2.9 wt %, ▼; 3.6 wt %, ◆; 4.5 wt %, +; 7.2 wt %, ×.

a stretched exponential function, $\Delta n'_{13} = \Delta n'_{13,0} \exp(-t/\tau)^{\beta}$ where the subscript 0 refers to the steady-state value and β is the shape parameter. The extracted relaxation times (τ) are displayed as a function of shear rate in Figure 6. We observe virtually the same value of τ for $c < 4.5$ wt %, although a weak decrease of τ from 0.1 to 0.07 s is observed in the shear rate range 10 s^{-1} < $\dot{\gamma}$ < 50 s^{-1}. The latter finding is correlated with a corresponding increase of β from about 0.6 to about 1 and attributed to the polydispersity of this sample. This behavior is consistent with the theory of Cates, according to which the number of clusters increases with concentration, rather than their size; therefore, the relaxation times should be essentially independent of the concentration. At higher concentrations, as gelation is approached, this argument does not hold any longer since clusters may be percolated and form larger entities which break up under the influence of shear.[5]

The magnitudes of the relaxation times confirm the presence of small clusters even at low concentrations, in harmony with earlier reports on the same systems.[5−7,13] At higher concentrations, a bimodal birefringence relaxation process is detected with the long relaxation times exceeding the fast ones by about 1 order of magnitude and attributed to the formation of large associations, as discussed in earlier investigations.[5,13] These times, for $c = 4.6$ and 7.2 wt %, exhibit a decrease with shear rate according to $\tau \sim \dot{\gamma}^{-0.5}$ (Figure 6).

III.3. Anisotropy in the Flow-Velocity Gradient Plane: Couette Experiments. a. Shear-Induced Birefringence. To probe the dynamics of the hairy-rod polyesters in the 12 plane (Scheme 2b), we used a Couette geometry, which also allowed detecting the flow-induced dichroism due to the long (compared to the parallel plates) optical path. Limitations in sample availability restricted these studies to only a few solutions. (This geometry is not suited for very concentrated solutions anyway, because of the enhanced viscosity and turbidity.) In particular, solutions in the semidilute regime $c^* < c < c^{**}$ were investigated. Their rheological properties are identical to those measured in the parallel plate geometry. Shear-induced birefringence was measured during step rate experiments at low concentrations, where it could not be resolved in the parallel plate geometry. Figure 7 depicts the shear rate dependence of the positive steady-state birefringence of a 0.5 wt % solution; it is apparent that $\Delta n'_{12}$ increases

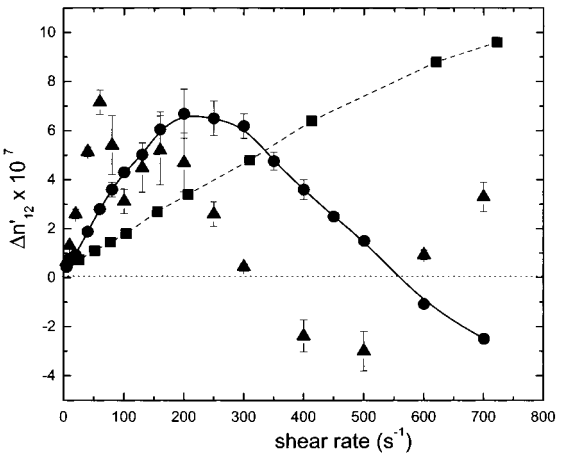

Figure 7. Shear rate dependence of the overall steady-state birefringence of semidilute TPPE solutions measured in the Couette geometry ($\Delta n_{12}'$): 0.5 wt %, ■; 0.7 wt %, ●; 1 wt %, ▲. Lines are drawn to guide the eye.

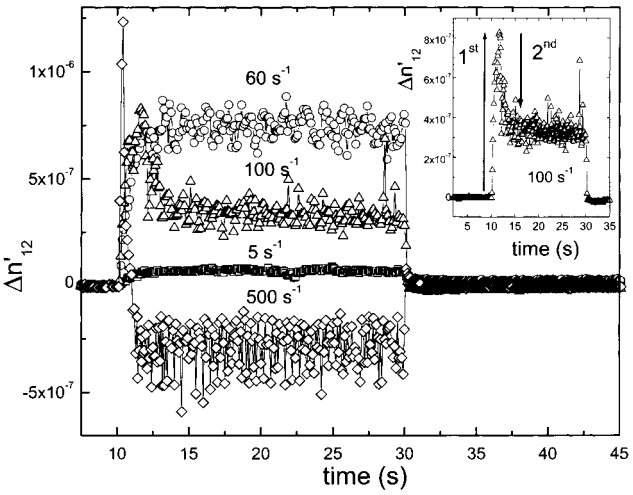

Figure 8. Transient birefringence $\Delta n_{12}'$ of 1 wt % TPPE solution at various shear rates (5−500 s^{-1}), indicating the change of sign with increasing rate. Inset: illustration of the two contributing birefringence processes for the case of $\dot{\gamma}$ = 100 s^{-1}.

monotonically with shear rate, whereas at the highest rates probed (500 < $\dot{\gamma}$ < 700 s^{-1}) a tendency toward saturation in the birefringence signal can be observed. Increasing the concentration to 0.7%, a transition in the sign of birefringence is detected with shear rate. Up to a shear rate value of about 200 s^{-1} an increasing positive $\Delta n'_{12}$ is detected; then $\Delta n'_{12}$ decreases and above 500 s^{-1} it becomes negative. The maximum in positive $\Delta n'_{12}$ is shifted to lower shear rates as the concentration increases to 1 wt % (Figure 7), and the transition to negative birefringence is probed above 300 s^{-1}; $\Delta n'_{12}$ goes through a minimum at $\dot{\gamma} \approx 500$ s^{-1}, and eventually it becomes positive again.

The change of sign of the overall shear-induced birefringence $\Delta n'_{12}$ is clearly manifested in the transients of Figure 8, for a concentration $c = 1$ wt %. At low shear rates, a single process associated with positive birefringence is probed (see data for $\dot{\gamma} = 60$ s^{-1}). As the shear rate increases, a second process (see down arrow in the inset of Figure 8, for $\dot{\gamma} = 100$ s^{-1}), exhibiting negative birefringence, is superimposed to the first process (up arrow in the inset); naturally, when the magnitude of the second process is larger than that of the first, the overall birefringence becomes negative.

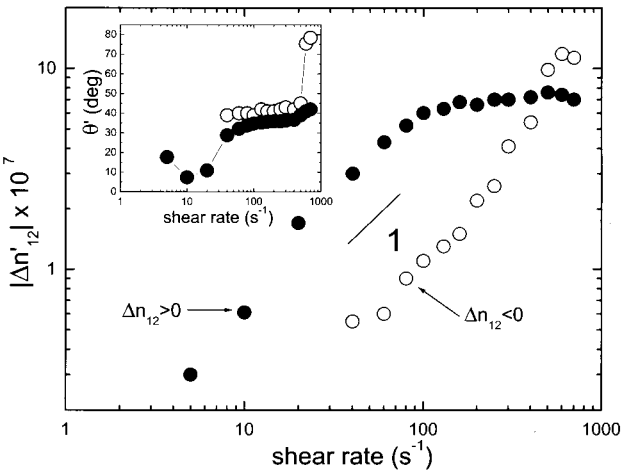

Figure 9. Shear rate dependence of the contributing processes to the overall flow birefringence $|\Delta n_{12}'|$ for a 0.7 wt % solution: fast positive process (●) and slow negative process (○). Inset: respective shear rate dependence of the birefringence orientation angles (θ').

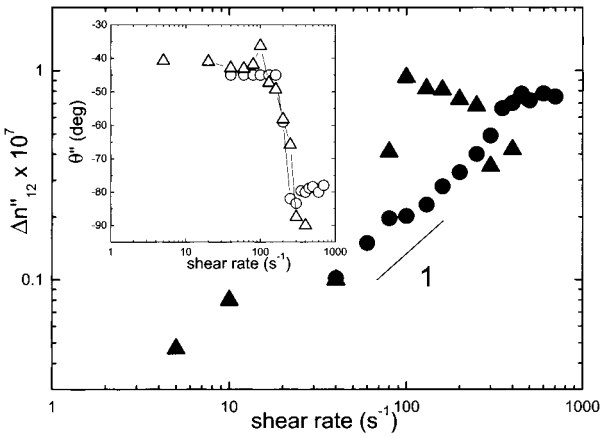

Figure 10. Shear rate dependence of the linear conservative dichroism $\Delta n_{12}''$ for two TPPE solutions: 0.7 wt % (●) and 1 wt % (▲). Inset: respective dichroism orientation angles (θ''): 0.7 wt % (○) and 1 wt % (△).

Scheme 3. Cartoon Illustration of the State of Orientation and Dynamics of Hairy Rod Polymer Solutions in Simple Shear Flow and at Different Concentration Regimes: (a) c < *c; (b) *c** < *c* < *c***; (c) *c* > *c*****

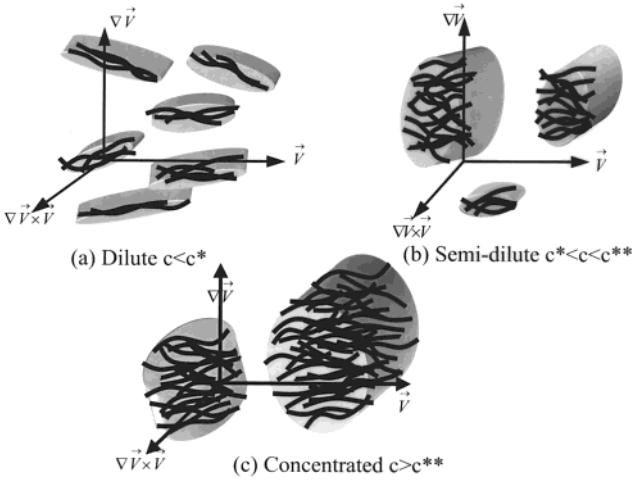

Note that the short time behavior in Figure 8 should be distinguished from the well-known overshoots, since the time at the peak of $\Delta n'_{12}$ does not scale with the imposed shear strain, as expected for flexible polymer solutions.[21]

From the analysis of the transients of Figure 8 the contributing processes to the overall birefringence signal can be extracted. Figure 9 depicts a typical example for a 0.7 wt % solution. Both a positive and a negative process are resolved, following roughly the scaling $|\Delta n_{12}'| \sim \dot{\gamma}$. At a shear rate value $\dot{\gamma} \approx 80$ s^{-1} the birefringence signal apparently levels off; however, this plateau is an experimental artifact since the rather long time resolution (50 ms) of the lock-in amplifiers makes it impossible to probe the true peak of the birefringence signal, which is the signature of the first process (see also inset of Figure 8). As such, this plateau will not be discussed further. Note that the second process associated with a negative birefringence is detected in the range 70 s^{-1} < $\dot{\gamma}$ < 400 s^{-1}, and only at the highest rates the scaling exponent seems to exceed unity. It is this increase of the birefringence of the second process that causes the transition of the overall $\Delta n'_{12}$ discussed above.[22]

The respective orientation angles of the two processes are shown in the inset of Figure 9. Whereas at low shear rates the first process orients practically along the flow direction (see also Scheme 2b), for $\dot{\gamma}$ > 10 s^{-1} it tends to a random orientation (45° with respect to the flow axis). This process is attributed to the trimers (which are actually the smallest-scale species[6]) which exhibit Newtonian behavior (Figure 1), in accord with similar studies on other wormlike polymer chains.[11,12] The fact that for $\dot{\gamma}$ < 10 s^{-1} the orientation angle goes to 0° is attributed to polydispersity in size of trimers and small clusters (steaming from the large molecular weight polydispersity of the synthesized polyesters as discussed in the experimental part); this is in qualitative agreement with the earlier investigations of Fuller and coworkers on the dynamics of polydisperse rodlike collagen proteins[11] and relevant theoretical models.[23] At small shear rates, the bigger trimers first orient since their associated rotational diffusivity is smaller (compared to the small trimers), and consequently the effective shear rate experienced by this population is higher than the effective shear rate experienced by the smaller trimers. This is consistent with the failure of the stress−optical rule at the lowest shear rates, as discussed below. The orientation of the clusters in the flow-vorticity plane (with their main axis along the velocity gradient direction as discussed below and illustrated in Scheme 3) is random at lower shear rates where it was detected[22] and becomes perpendicular to the flow direction as shear is enhanced. Note that the absence of shear thickening excludes the possibility of strong aggregation under flow.

b. Emergence of Dichroism. Figure 10 illustrates the linear conservative dichroism $\Delta n_{12}''$ probed for sheared 0.7% and 1 wt % solutions; its magnitude is 1 order of magnitude smaller than the corresponding birefringence (Figure 9). The fact that roughly $\Delta n_{12}'' \sim \dot{\gamma}$ may be suggestive of the same origin of the negative birefringence (Figure 9) and dichroism (clusters); note that only one process was resolved by the dichroism signal, which is positive. The orientation angle of the dichroism, θ'', is shown in the inset of Figure 10; whereas at low shear rates a random orientation of $\Delta n''$ is observed, above 100 s^{-1} the principal axis of dichroism is oriented perpendicular to the flow, much like the negative birefringence attributed to the clusters (see

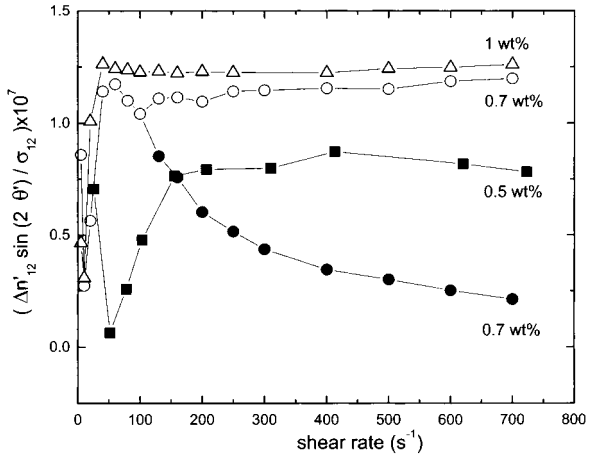

Figure 11. Examination of the validity of the stress−optical rule in a plot of $\Delta n_{12}' \sin(2\theta')/\sigma_{12}$ vs $\dot{\gamma}$ for different concentrations: 0.5 wt % (■), 0.7 wt % (●, ○), and 1 wt % (△). The open symbols refer to the calculation of the stress−optical ratio from the extrapolation of the first birefringence process (see text).

also inset of Figure 9). Therefore, the emergence of scattering dichroism reveals the presence of clusters, which orient along the velocity gradient and give rise to a negative birefringence as well with the same orientation behavior.

It is noted that the positive $\Delta n_{12}'$ probed for the more dilute solutions of 0.5 and 0.7 wt % exhibits the same orientation characteristics with the positive process of the 1 wt % solution (Figures 8 and 9); in other words, θ' orients along the flow direction at lower shear rates and is randomized at higher shear rates. This result is in agreement with the orientation behavior reported by Gatzonis et al.;[12] in that case these results were explained with the presence of two populations, single molecules with $\theta' = 45°$ and clusters orienting on the flow direction. The cartoons of Scheme 3 attempt to represent the response of the investigated TPPE's to the simple shear flow imposed, in the whole concentration range. Briefly, at low concentrations the polydisperse trimers orient along the flow; in the semidilute regime polydisperse clusters are formed, in equilibrium with some free trimers, which are along the vorticity direction, but with their constituent chains along the flow direction; in the concentrated region these phenomena are enhanced with large clusters dominating the dynamics of this effective suspension. The low concentration regime was actually resolved with the Couette experiments, whereas the parallel plate experiments were used to document the high concentration regime. The key features here include a negative birefringence (and positive dichroism), due to the clusters, in the vorticity−velocity gradient plane, and a positive birefringence, due to the trimers, in the flow direction.

c. Stress−Optical Rule. Figure 11 tests the validity of the stress−optical rule for the 0.5%, 0.7%, and 1 wt % solutions by plotting $\Delta n_{12}' \sin(2\theta')/\sigma_{12}$ vs $\dot{\gamma}$. The extracted values of the stress−optical coefficient C are consistent with the analysis presented for the parallel plate geometry in the 13 plane (Figure 5) and further confirm that the TPPE species (trimers) are essentially semiflexible.

For the 0.7 wt % solution, the use of the first process (positive birefringence) as extracted from the transients leads to a ratio $\Delta n_{12}' \sin(2\theta')/\sigma_{12}$, which is shear rate dependent. This stems from the fact that the first process saturates at higher shear rates, due to the experimental artifact described above in reference to Figure 9. Extrapolating the first process from the data collected at small shear rates, where the overshoots are resolved without experimental troubles, and using these extrapolated values in the stress−optical ratio, enables us to obtain the curve with open circles of Figure 11. This curve demonstrates that the stress−optical rule (SOR) is verified with a corresponding stress−optical coefficient C of about 1.15×10^{-7} Pa^{-1}. This result (SOR validity) is in harmony with the Newtonian behavior probed with the rheology. Using this analysis, the stress−optical coefficient C for the 1 wt % solution was found to be 1.25×10^{-7} Pa^{-1}. The 0.5 wt % solution, also shown in Figure 11, has a single birefringence mode and yields $C \approx 0.75 \times 10^{-7}$ Pa^{-1}; from the examination of these three concentrations it is seen that C exhibits a weak concentration dependence. It should be noted that C is independent of concentration for flexible macromolecules.[10]

Interestingly, the SOR is seen not to hold in the low shear rate regime. Polydispersity in trimers sizes (due to large polydispersity in molecular weight of the TPPE's) is proposed as the origin of the SOR failure.[11,17] At low shear the larger trimers orient whereas the smaller remain practically randomized, and no SOR is obtained; on the other hand, at higher shear rates all trimers are aligned in the flow direction, and thus the SOR is essentially recovered with a corresponding stress−optical coefficient C characteristic of this trimer population. A final observation relates to the range of shear rates in which the SOR is violated. Apparently, it depends on concentration, being smaller and shifting to smaller shear rate values as the concentration increases.

IV. Concluding Remarks

The shear response of hairy-rod polyester solutions above c^* can be investigated using in-situ optical rheometry in both the flow-vorticity and flow-velocity gradient planes. The transition from the semidilute to the concentrated regime, c^{**}, is characterized by a strong concentration dependence of the zero shear viscosity, a change in the sign of birefringence, and the emergence of linear conservative dichroism. These results can be compiled in the cartoon of Scheme 3, which attempts to illustrate the orientation and aggregation of the hairy-rod solutions at various concentration regimes. The underlying finding is the presence of anisotropic clusters which dominate the dynamics at the higher concentrations and can be identified by the changing sign of birefringence and emergence of dichroism. They are oriented perpendicular to the flow and with their main axis along the velocity gradient direction, with constituent species (trimers) following the flow.

The stress−optical rule is found to hold only in the concentration regime below c^{**}, where trimers represent the essential constituents of the solutions, yielding stress−optical coefficients typical of wormlike polymers. The anomalous birefringence (change of sign) can be rationalized using the theoretical analysis of Cates, who considered a presmectic local ordering resulting from the interplay of sterically interacting particles and the external field, and is consistent with earlier studies on other associating wormlike systems.

References and Notes

(1) Russo, P. S. In *Dynamic Light Scattering. The Method and Some Applications*; Brown, W., Ed.; Oxford University Press: New York, 1993. Tracy, M. A.; Pecora, R. *Annu. Rev. Phys. Chem*. **1992**, *43*, 525.

(2) Sato, T.; Teramoto, A. *Adv. Polym. Sci*. **1996**, *186*, 85.

(3) Wegner, G. *Macromol. Symp*. **1996**, *104*, 29. Ober, C. K.; Wegner, G. *Adv. Mater*. **1997**, *9*, 17. Müllen, K. Wegner, G. *Adv. Mater*. **1998**, *10*, 433. Baum, P.; Meyer, W. H.; Wegner, G. *Polymer* **2000**, *41*, 965.

(4) Andrikopoulos, K.; Vlassopoulos, D.; Voyiatzis, G.; Yiannopoulos, E.; Kamitsos, E. I. *Macromolecules* **1998**, *31*, 5465.

(5) Hilliou, L.; Vlassopoulos, D.; Rehahn, M. *Rheol. Acta* **1999**, *38*, 514.

(6) Petekidis, G.; Vlassopoulos, D.; Fytas, G.; Kountourakis, N.; Kumar, S. *Macromolecules* **1997**, *30*, 919.

(7) Petekidis, G.; Vlassopoulos, D.; Fytas, G.; Rulkens, R.; Wegner, G. *Macromolecules* **1998**, *31*, 6129. Petekidis, G.; Vlassopoulos, D.; Fytas, G.; Rulkens, R.; Wegner, G.; Fleischer, G. *Macromolecules* **1998**, *31*, 6139. Petekidis, G.; Vlassopoulos, D.; Fytas, G.; Fleischer, G. *Macromolecules* **1998**, *31*, 1406.

(8) Petekidis, G.; Vlassopoulos, D.; Galda, P.; Rehahn, M.; Ballauff, M. *Macromolecules* **1996**, *29*, 8948.

(9) Rehahn, M.; Schluter, A. D.; Wegner, G. *Makromol. Chem*. **1990**, *191*, 1991. Kallitsis, J. K.; Rehahn, M.; Wegner, G. *Makromol. Chem*. **1992**, *193*, 1021. Tiesler, U.; Pulina, T.; Rehahn, M.; Ballauff, M. *Mol. Cryst. Liq. Cryst*. **1994**, *243*, 299.

(10) Fuller, G. G. *Optical Rheometry of Complex Fluids*; Oxford University Press: New York, 1995.

(11) Chow, A. W.; Fuller, G. G.; Wallace, D. G.; Madri, J. A. *Macromolecules* **1985**, *18*, 793. Chow, A. W.; Fuller, G. G.; Wallace, D. G.; Madri, J. A. *Macromolecules* **1985**, *18*, 805. Meyer, E. L.; Fuller, G. G.; Clark, R. C.; Kulicke, W.-M. *Macromolecules* **1993**, *26*, 504.

(12) Gatzonis, Y.; Siddiquee, S. K.; van Egmond, J. W. *Macromolecules* **1997**, *30*, 7253. Siddiquee, S. K.; van Egmond, J. W. *Macromolecules* **1998**, *31*, 2661.

(13) Hilliou, L.; Vlassopoulos, D.; Rehahn, M. *Macromolecules* **2000**, *33*, 3105.

(14) Cates, M. E. *J. Phys. II* **1992**, *2*, 1109.

(15) Doi, M.; Edwards, S. F. *The Theory of Polymer Dynamics*; Oxford University Press: New York, 1986.

(16) Petekidis, G.; Vlassopoulos, D.; Fytas, G.; Fleischer, G.; Wegner, G. *Macromolecules* **2000**, *33*, 9630.

(17) Mead, D. W.; Larson, R. G. *Macromolecules* **1990**, *23*, 2524.

(18) Hilliou, L.; et al., unpublished data.

(19) Oda, R.; Lequeux, F.; Mendes, E. *J. Phys. II* **1996**, *6*, 1429. Narayanan, J.; Mendes, E.; Manohav, C. *J. Phys. Chem*. **1996**, *100*, 18524.

(20) Chu, S. G.; Venkatraman, S.; Berry G. C.; Einaga, Y. *Macromolecules* **1981**, *14*, 939.

(21) Larson, R. G. *Constitutive Equations for Melts and Solutions*; Butterworth: Boston, 1988.

(22) At low shear rates $\dot{\gamma} < 70\ s^{-1}$ the negative contribution to the overall $\Delta n'_{12}$ is not resolved because of the small amount of clusters (giving rise to the negative birefringence) at this concentration of 0.7 wt %. Therefore, whereas clusters do orient first at lower shear due to their reduced rotational diffusivity, their optical signal (and thus detection) is much weaker compared to the more anisotropic trimers.

(23) Marrucci, G.; Grizzuti, N. *J. Polym. Sci., Polym. Lett. Ed*. **1983**, *21*, 83. Marrucci, G.; Grizzuti, N. *J. Non-Newtonian Fluid Mech*. **1984**, *14*, 13.

MA001917L